Direct Observation of Zeolite A Synthesis by in Situ Solid-State NMR

Jimin Shi and Michael W. Anderson

Department of Chemistry, UMIST, P.O. Box 88, Manchester, M60 1QD, UK

Stuart W. Carr*,†

Unilever Research, Quarry Road East, Bebington, Merseyside, L63 3JW, UK

Received January 17, 1995. Revised Manuscript Received October 26, 1995[⊗]

This paper describes the use of in situ solid-state NMR and X-ray powder diffraction to study the real-time synthesis of zeolite A. In particular ^{27}Al and ^{29}Si are used to monitor the growth of the crystalline phase and the species which occur in solution and the gel phases. A parallel in situ X-ray diffraction study was used to investigate the development of long-range order of the material. Conclusions concerning the mechanism of the formation of zeolite A are proposed.

Introduction

Zeolites are unique materials with well-defined microporous structures of molecular dimensions.[1] This arises because of subtle variations in channel and/or pore size and differences in connectivity. Small changes can lead to significant changes in the properties of a particular structural type. The zeolite aluminosilicates are built from simple tetrahedral SiO_4 and AlO_4 units, and their unique properties are determined by the range of different ways of connecting these units. Given the simplicity of these units, it is surprising that such complex structures can self-assemble in "one-pot reactions" from multiphase mixtures. The formation of a particular structure is very sensitive to the exact composition and nature of the species present in the precursor gel. The lack of understanding of the synthesis of zeolites has led to a large amount of empirical experimentation with the aim of generating new structural types.[2]

Two mechanisms of zeolite formation from these multiphasic mixtures have been postulated, one based on a liquid-phase transformation mechanism and the second ascribed to a solid hydrogel transformation.[1] The crystallization kinetics have been studied for a number of zeolites, and the classic S-shaped growth curve is observed.[3] The methodology involves using representative crystallite size as a measure of the rate of crystal growth. In the case of zeolite A a more detailed analysis enabled the nucleation and growth curves to be calculated under a range of synthesis conditions.[4−7] Over a number of years Thompson et al.[6] have developed mathematical models to study zeolite crystallization and nucleation behavior using the population balance model. Chen et al.[7] describe a similar approach. Both groups claim good agreement between experimental and calculated growth curves. However, these approaches suffer from a lack of detailed understanding of the key nucleation and growth processes at a chemical level. More recently an empirical model based on a detailed study of the nucleation and growth of zeolite 4A has been published.[4,5]

There have been a number of studies using a variety of techniques in an attempt to gain a detailed understanding of the processes which occur during synthesis.[1,8−10] A constant theme in these studies has been to relate the observed nucleation and growth behavior to the changes in nature of the aluminate, silicate, and aluminosilicate speciation with the objective of building a molecular picture of the zeolite formation process.[11] NMR studies have found utility in the study of zeolite formation because it is possible to gain detailed information about speciation for both solid and solution phases as well as relative degree of crystallization.[10] It is especially powerful when used in conjunction with other techniques such as X-ray powder diffraction. Several groups have used NMR to study the precursors in the solid and solutions phases of the zeolite gels. In one of the earliest studies Engelhardt et al. studied the ^{29}Si and ^{27}Al NMR of the separated solid phase of zeolite A as a function of crystallization and the source of silicate and aluminate.[12,13] It was found that the initial sources greatly affected the intermediates observed but not the final zeolite A product. These studies have been extended to a number of zeolite systems, for example

† Current address: ICI Explosives−Technical, P.O. Box 196, Kuni Kuni, NSW 2327, Australia.

⊗ Abstract published in *Advance ACS Abstracts*, December 1, 1995.

(1) Barrer, R. M. *Hydrothermal Synthesis of Zeolites*; Academic Press: 1982, London.

(2) Davis, M. E.; Lobo, R. F. *Chem. Mater.* **1992**, *4*, 756−768 and references therein.

(3) Zhdanov, S. P.; Khvoshcheu, S. S.; Feoktistova, N. N. *Synthetic Zeolites*; Gordon and Breach: New York, 1990; Vol. 1.

(4) Myatt, G. J.; Budd, P. M.; Price, C.; Hollway, F.; Carr, S. W. *Zeolites* **1994**, *14*, 190−197.

(5) Budd, P. M.; Myatt, J.; Price, C.; Carr, S. W. *Zeolites* **1994**, *14*, 198−202.

(6) Thompson, R. W. In *Modelling of Structures and Reactivity in Zeolites*; Catlow, C. R. A., Ed.; Academic Press: London, 1994.

(7) Chen, W. H.; Hu, H. C.; Lee, T. Y. *Chem. Eng. Sci.* **1993**, *48*, 3683.

(8) Engelhardt, G.; Michel, D. *High-Resolution NMR of Silicate and Zeolites*; John Wiley & Sons Ltd.: New York, 1987.

(9) McCormick, A. V.; Bell, A. T. *Catal. Rev. Sci. Eng.* **1989**, *31*, 97−127.

(10) Swaddle, T. W.; Salerno, J.; Tregloan, P. A. *Chem. Soc. Rev.* **1994**, *23*, 319−326.

(11) Davis, M. E. *ACS Symp. Ser.* **1994**, *561*, 26−37.

(12) Engelhardt, G.; Fahlke, B. *Zeolites* **1983**, *3*, 292.

(13) Engelhardt, G.; Fahlke, B.; Magi, M.; Lippmaa, E. *Zeolites* **1985**, *5*, 49.

0897-4756/96/2808-0369$12.00/0 Published 1996 by the American Chemical Society

Table 1

gel	solution A	solution B	aging conditions[a]
1	8.33 g of sodium aluminate solution + 167 H_2O + 2.5 g NaOH	6.5 g of sodium silicate + 20.83 g of H_2O	stirring for 30 min
2	8.5 g of sodium aluminate solution	6.65 g of sodium silicate + 3.24 g of H_2O	stirring for 30 min

[a] Time before placing in the NMR rotor or onto the XRD stage. For the XRD and NMR experiments data were collected for samples prepared individually and for experiments in which the gel was divided. The results were essentially the same.

Y,[14−17] mordenite,[15,18] hydroxysodalite,[19] ZSM5,[20−25] and zeolite A.[26] However all these studies have been undertaken on either systems in which the solid and solution phase have been separated and analyzed independently or the gels have been quenched and analyzed ex situ. The purpose of this paper is to demonstrate that magic-angle spinning NMR techniques can be applied to the in situ study of zeolite synthesis and that it can be used to follow the speciation as a function of time. Zeolite A was chosen as a model system as its crystallization behavior is well established and its crystallization time and conditions are reasonable.[4,5,12,13,26] Two gels with the same aluminate and silicate composition but differing water and alkali contents were chosen for study as recent studies have shown that the nucleation and growth behavior was significantly different.[4] To complement the NMR work, X-ray diffraction was used to monitor the crystallization process and to confirm the nature of the final products.

Experimental Section

Gel Preparation. The preparation of the zeolite gels essentially follows our previous publication.[4] Sodium silicate (SiO_2 20%, Na_2O 12%), sodium aluminate (Al_2O_3 20%, Na_2O 20%), and NaOH were obtained from BDHL, Laporte, and Aldrich, respectively, and were used as received. Two gel compositions were chosen for study. These were follows:

Gel 1 Al_2O_3:2SiO_2:4.3Na_2O:160H_2O

Gel 2 Al_2O_3:2SiO_2:2.4Na_2O:42H_2O

The gels were prepared as described in Table 1 and aged at 75 and 65 °C for gels 1 and 2, respectively.

The synthesis gels were prepared by adding solution A to B with vigorous stirring with a paddle stirrer until a homogeneous gel had formed.

In Situ XRD. In situ X-ray diffractograms on a zeolite-A synthesis were recorded at an interval of 6 min with continuous scanning at 2θ = 10°/min on a SCINTAG DMS-2000 spectrometer using flatplate geometry. The synthesis gel was put in the copper sample holder which was covered by PTFE film (clingfilm) to prevent water from evaporating during aging at 65 °C. The background from the clingfilm cover was subtracted from all diffraction patterns.

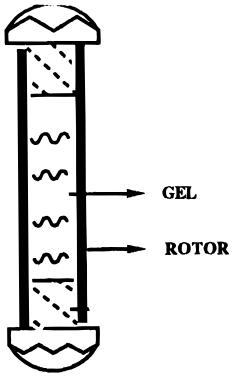

Figure 1. Diagram illustrating the method used to seal the zeolite A gels in rotors.

In Situ ^{29}Si and ^{27}Al MAS NMR. The ^{27}Al and ^{29}Si MAS NMR spectra were collected on a Bruker MSL-400 solid-state spectrometer using a Chemagnetics Probe. The gel was put into a 7 mm Chemagnetics rotor sealed with Teflon end caps at room temperature and heated at the desired temperatures with nitrogen gas flow. Samples were sealed in the rotor as per Figure 1. The rotor was spun at a speed of 2100 Hz using nitrogen gas. The ^{27}Al spectra were recorded at 10 min intervals with 3000 scans. Single pulse mode was used with 200 ms repetition time, 0.6 μs pulse width. Chemical shifts are quoted relative to the $[Al(H_2O)_6]^{3+}$ as standard.

^{29}Si MAS NMR spectra were collected in single-pulse mode with 2 s repetition time, 2 μs pulse width at an interval of 14 min, and 400 scans. Chemical shifts are referred to TMS as standard.

Results

Characterization of the Final Products. *Solid-State NMR.* Figure 2 shows selected ^{29}Si and ^{27}Al MAS NMR spectra of the final product of zeolite A made from both gels 1 and 2 in and out of the rotor. They all have similar lineshapes. The half-height width of the peaks in the ^{29}Si MAS NMR ($\Delta\nu_{1/2}$ = 140 Hz) and ^{27}Al MAS NMR spectra ($\Delta\nu_{1/2}$ = 400 Hz) are similar. Preparation in the NMR rotor or in the XRD diffraction sample holder does not affect the nature of the final product. In gels 1 and 2 a small amount of zeolite X is observed.

Scanning Electron Microscopy. Figures 3 and 4 show the scanning electron micrographs (SEM) of zeolite-A synthesized using gels 1 and 2, respectively. All have the typical cubic morphology of zeolite A. Close examination of the image taken from the sample made from gel 1 indicates that some of the cubic crystals are twinned with a small number of octahedral crystals, typical of zeolite X. The crystals of zeolite A made from recipe 2 in both the oven and the copper XRD holder are very similar in size (about 0.5 μm), but they are larger than those made in the rotor (Figure 4a). This difference could be due to the effect of sample spinning on nucleation and crystal growth behavior.

(14) Dewale, N.; Bodart, P.; Gabelica, Z.; Nagy, J. B. *Acta Chim. Acad. Sci. Hung.* **1985**, *119*, 233.
(15) Bodart, P.; Nagy, J. B.; Gabelica, Z.; Derouane, E. G. *J. Chim. Phys. Chim. Biol.* **1986**, *83*, 777.
(16) Thangaraj, A.; Kumar, R. *Zeolites* **1990**, *10*, 117−120.
(17) Kasahara, S.; Itabashi, K.; Igawa, K. *Stud. Surf. Sci. Catal.* **1986**, *28*, 185−192.
(18) Bodart, P.; Gabelica, Z.; Nagy, J. B.; Debras, G. In *Zeolites: Science and Technology*; Ribeiro, R. F., et al., Eds.; Martinus Nijhoff: Den Hagg, 1984; p 211.
(19) Hayashi, S.; Suzuki, K.; Shin, S.; Hayamizu, K.; Yamamoto, O. *Chem. Phys. Lett.* **1985**, *113*, 368.
(20) Gabelica, Z.; Nagy, J. B.; Debras, G.; Derouane, E. G. In *Proceedings of the 6th International Zeolite Conferences (Reno, 1984)*; Butterworth: Guildford, 1980; p 914.
(21) Gabelica, Z.; Nagy, J. B.; Debras, G.; Derouane, E. G. *Acta Chim. Acad. Sci., Hung.* **1985**, *119*, 275.
(22) Burkett, S. L.; Davis, M. E. *J. Phys. Chem.* **1994**, *98*, 4647−4653.
(23) Burkett, S. L.; Davis, M. E. *Chem. Mater.* **1995**, *7*, 920−928.
(24) Chang, C. D.; Bell, A. T. *Catal. Lett.* **1991**, *8*, 305−316.
(25) Gittleman, C. S.; Bell, A. T.; Radke, C. J. *Micropor. Mater.* **1994**, *2*, 145−158.
(26) Tsuruta, Y.; Satoh, T.; Yoshida, T.; Okumura, O.; Ueda, S. Studies on the Initial Product in the Synthesis of Zeolite A from Concentrated Solution; Proceedings of the 7th Zeolite International Conference, Tokyo, 1976; p 1001.

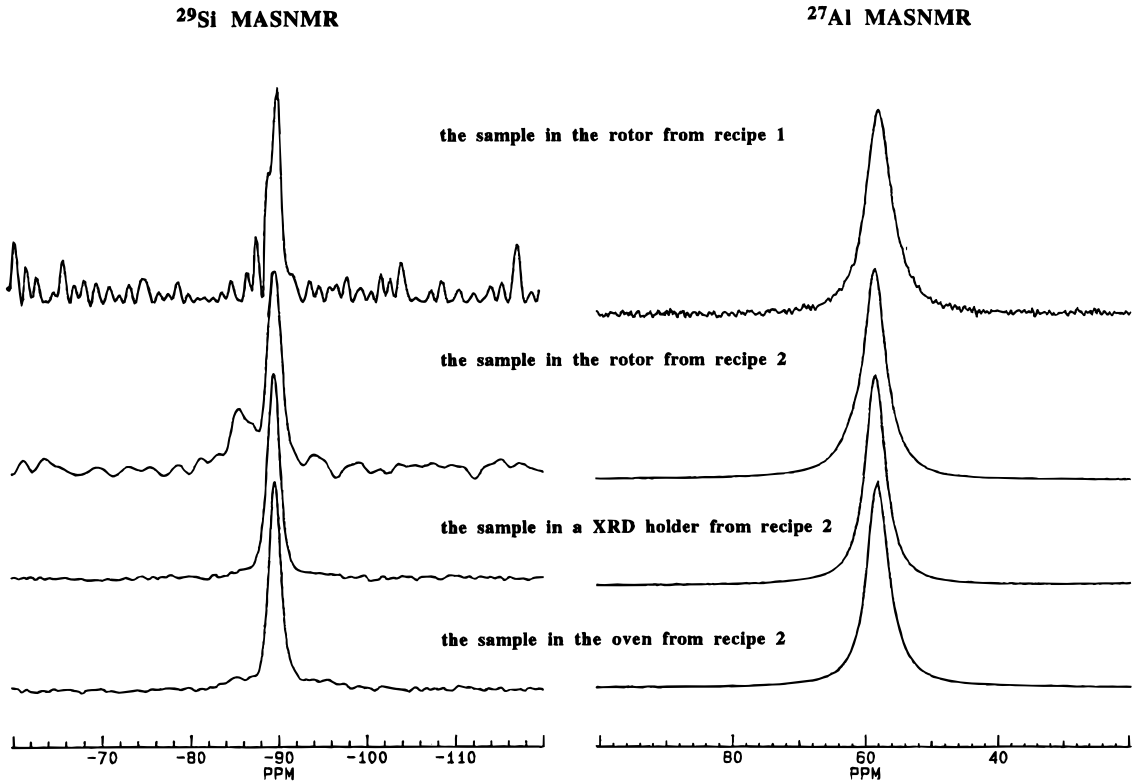

Figure 2. ^{29}Si MAS NMR and ^{27}Al MAS NMR spectra of the final products of a typical zeolite A synthesis made by gels 1 and 2.

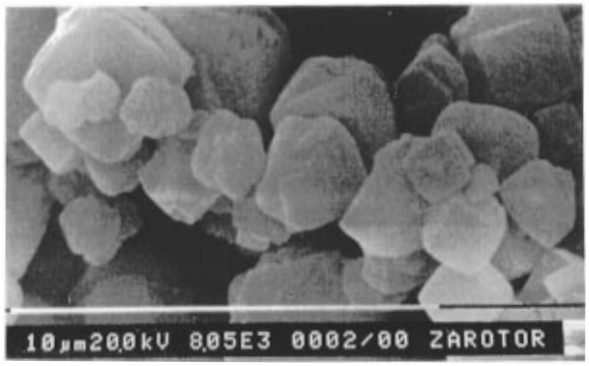

8000 x sample made in the rotor of NMR spectrometer

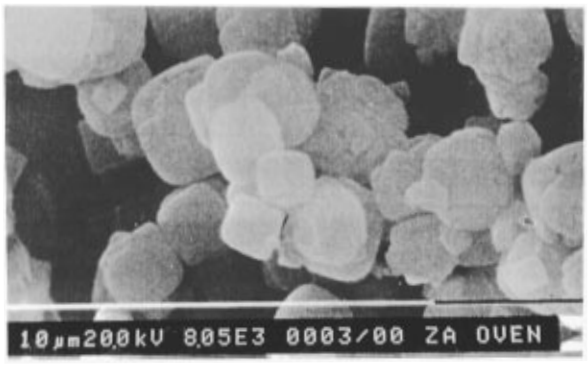

8000 x sample made in the oven

Figure 3. SEM photographs of zeolite A made from gel 1 at 75 °C for 4.5 h prepared in (top) the NMR machine and (bottom) in a conventional unstirred synthesis.

XRD. XRD patterns of the products (gels 1 and 2) prepared in the NMR rotor, in the XRD holder, and in the oven are shown in Figure 5. The X-ray diffraction patterns indicate that all products are highly crystalline zeolite A. In some examples a small zeolite X impurity was observed (gels 1 and 2, rotor and normal hydrothermal synthesis).

In Situ Measurements. *XRD.* In situ X-ray powder diffraction patterns were recorded from gel 2 as shown in Figure 6. The half-height of the peak at $2\theta = 29.94°$ ($hkl = 410\ 322$) vs heating time was measured, and the curve is shown in Figure 12. In the initial 30 min, XRD patterns show that the aluminosilicate gel consists of amorphous material. This stage can be assigned to the induction and nucleation period. The diffraction lines began to appear after 36 min, indicating the presence of X-ray observable crystals.

These correspond to zeolite A (Table 2). As crystallization proceeds, diffraction lines become narrower and increase in intensity, indicating a rapid increase in crystallinity.

^{29}Si MAS NMR Spectra. Figure 7 shows the ^{29}Si MAS NMR spectrum of the zeolite A gel obtained from gel 1 before heating. The peak at −72 ppm is assigned to Q^0 silicate species,[6] and the broad resonance in the range between −75 and −95 ppm is attributed to a complex mixture of Si(0Al), Si(1Al), Si(2Al), Si(3Al), and Si(4Al) aluminosilicate species. It is not possible to rule out the presence of Q^1, Q^2, and Q^3 silicate species. The broadness of this resonance is probably caused by overlapping broad peaks with slightly different δ values due to small differences in structural arrangement of SiO_4 tetrahedra in the gel skeleton and to second nearest-neighbor effects.[8] The peak at −103 ppm is assigned to Q^4 silicate species. The ^{29}Si MAS NMR of the gel 2 before heating (Figure 8) gives a specrum similiar to that of gel 1. The main difference between the two gels are the water and NaOH content which alters the speciation of the gel slightly—that is, more Q^0 for Gel 1.

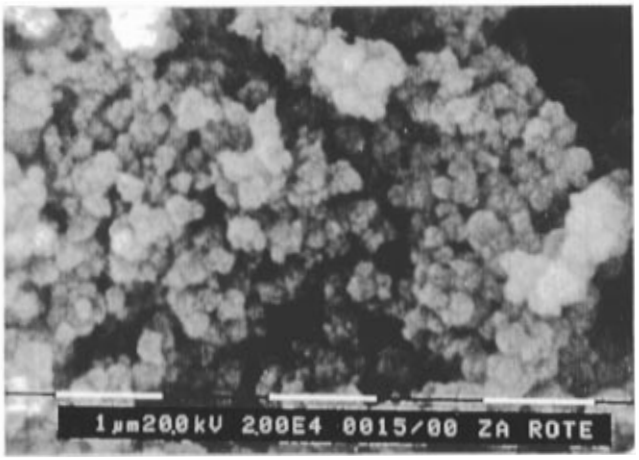

20,000 x sample made in the rotor of NMR spectrometer

20,000 x sample made in the copper holder of XRD diffratometer

20,000 x sample made in the oven

Figure 4. SEM photographs of zeolite A made from gel 2 at 65 °C for 4 h prepared in (top) the NMR spectrometer, (middle) the X-ray diffractometer, and (bottom) a conventional unstirred synthesis.

Figure 8 shows the in situ ^{29}Si MAS NMR spectra of the synthesis of zeolite A (gel 2) at 65 °C. For the first 40 min after heating there is little apparent change in the spectra. This period of crystallization of zeolite A has been ascribed to induction and nucleation.[4,5] Thus the in situ NMR experiment does not provide information about these events. This suggests that the rearrangements occurring in the gel are either too small to be observed by NMR or that the changes are occurring in the longer range order of the gel.

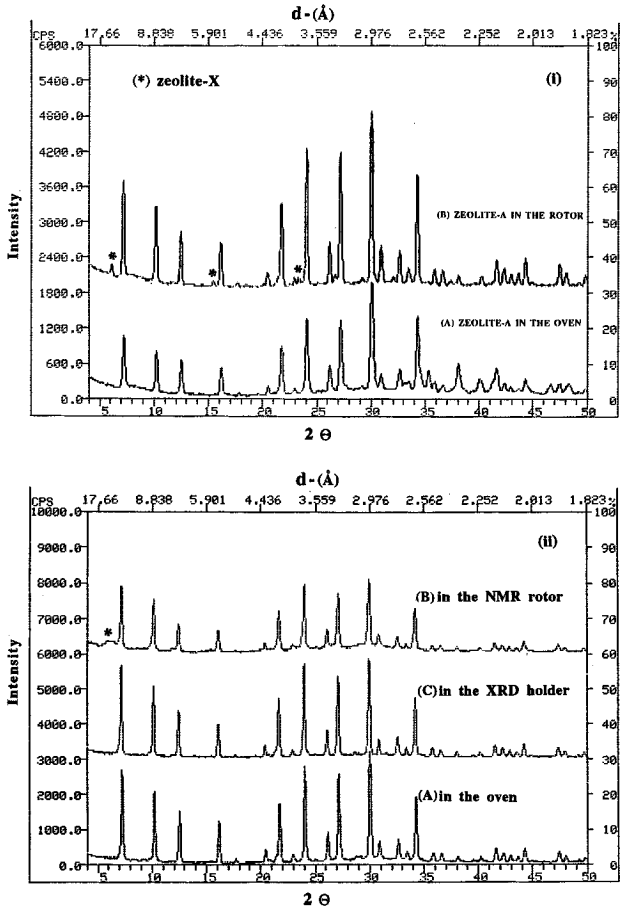

Figure 5. X-ray diffractograms of zeolite A prepared from gel 1 (i) and gel 2 (ii) in the NMR rotor and SRD holder and in a conventional synthesis [* indicates zeolite X impurity].

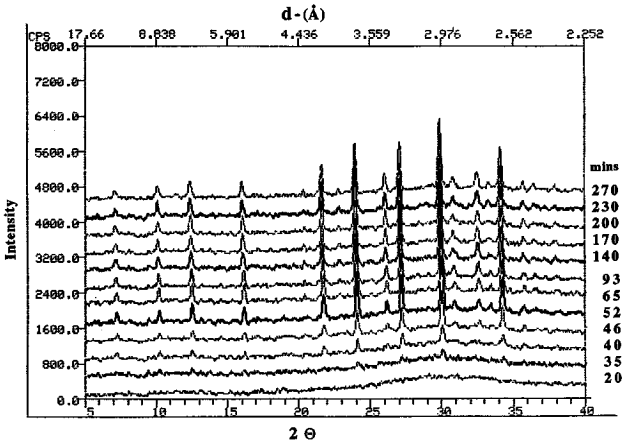

Figure 6. In situ XRD diffractograms on a zeolite A synthesis from gel 2 aged at 65 °C (after 30 min of mixing).

In the 40−70 min period it is possible only to tentatively assign the resonance due to zeolite A although it is clearly seen in the complementary XRD experiments. The small resonance at −85 ppm is assigned to a zeolite X impurity as observed in the XRD patterns. Figure 9 shows the curve of half-height width of the peak at the −89 ppm vs heating time (after 100 min) obtained from the ^{29}Si MAS NMR spectra of gel 2. The decreasing half-height width from 100 to 150 min indicates an ordering of the local environment about the

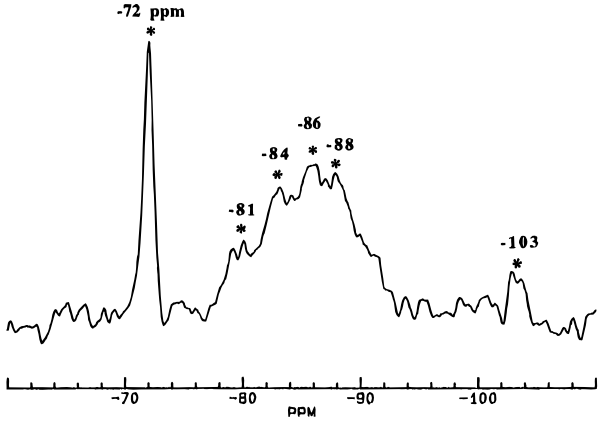

Figure 7. ^{29}Si MAs NMR spectrum of zeolite A synthesis gel from gel 1 at room temperature.

Table 2. Diffraction Lines Observed in the XRD Diffractogram after the Synthesis Gel with Recipe 2 Was Heated for 36 Min

2θ	d (Å)	h	k	l
7.53	11.73	2	0	0
10.52	8.41	2	2	0
12.80	6.91	2	2	2
16.45	5.39	4	2	0
22.01	4.03	4(6)	4(0)	2(0)
24.35	3.65	6	2	2
27.45	3.25	6	4	2
29.94	2.95	6(8)	4(2)	4(0)
34.52	2.60	6	6	4

silicon tetrahedra which suggests a rapid increase in crystallinity. After 150 min the constant half-height width indicates an ordered silicon environment exists and corresponds to a period of crystal growth. There is good correlation with data for the half-height width of the peak at $2\theta = 29.9°$ vs heating time from the X-ray diffractograms with gel 2 (Figure 12). A small and approximately constant amount of Q^0 silicate is observed throughout the synthesis. It was not possible to perform a ^{29}Si in situ NMR experiment with gel 1 because of the poor signal-to-noise of the more dilute gel. The required aquisition time for one spectrum was too long to obtain a reasonable picture of the synthesis process.

^{27}Al MAS NMR Spectra. The ^{27}Al MAS NMR spectra for zeolite A synthesis or gels 1 and 2 are shown in Figures 10 and 11, respectively. Each has two resonances (59, 78 ppm). The former is attributed to aluminosilicate units, that is, tetrahedrally coordinated aluminum linked by oxygen bridges to silicon and the latter to soluble $[Al(OH)_4]^-$. The ^{27}Al MAS NMR spectra reflect the observations made from the ^{29}Si NMR data. In gel 1 there is more free $[Al(OH)_4]^-$ and more $[Si(OH)_4]$ (see above). The $w_{1/2}$ of the aluminosilicate resonance is broader for gel 2. The $[Al(OH)_4]^-$ band decreases in intensity as the free aluminum is incorporated into the zeolite.

A plot of the width at half-height of the peak at about +59 ppm against heating time is shown in Figure 12. The reduction in half-width as the crystallization proceeds is assigned to the formation of crystalline zeolite A.[9,10] The concentration of aluminum as $[Al(OH)_4]^-$ ions in the liquid phase and that of aluminum as $Al(OSi)_4$ units in the solid phase vs the heating time are also shown in Figure 12.

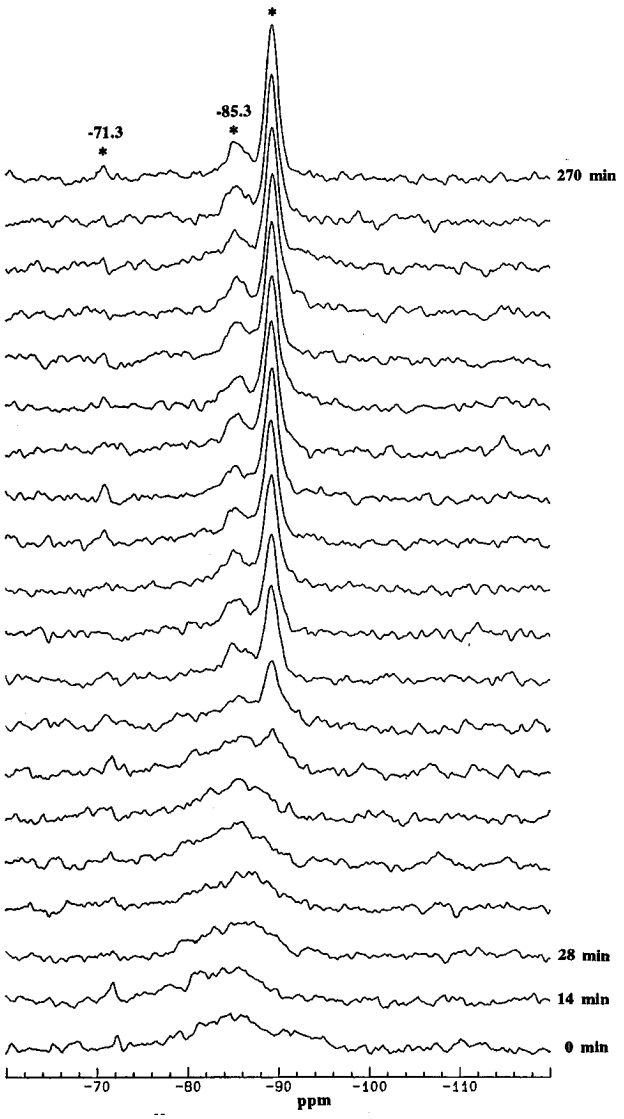

Figure 8. In situ ^{29}Si MAS NMR spectra of zeolite A synthesis from gel 2 at 65 °C, each spectrum was collected at an interval of about 14 min (after 30 min of mixing).

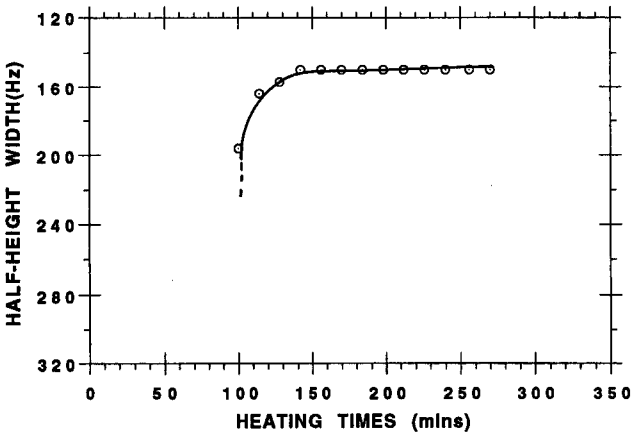

Figure 9. Plot of the half-height width of the peak at −89 ppm vs heating time (gel 2).

The most dramatic changes in the ^{27}Al NMR corresponds to increasing crystallinity (also from XRD and ^{29}Si NMR). The initiation of crystal growth is relatively independent of composition in these experiments despite the presence of very different species. Crystal growth starts between 40 and 50 min. This behavior is con-

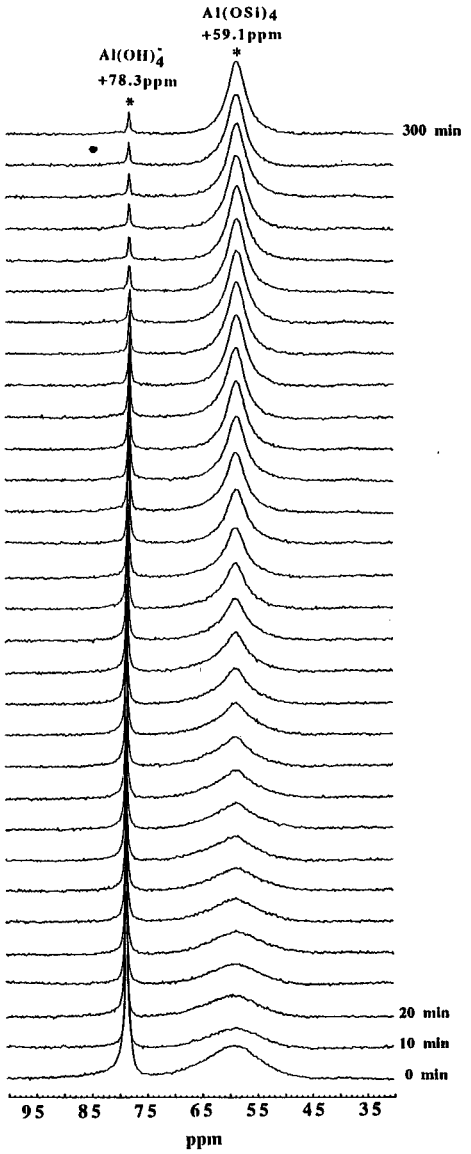

Figure 10. In situ ^{27}Al MAS NMR spectra on a zeolite A synthesis from gel 1 at 75 °C (after 30 min of mixing).

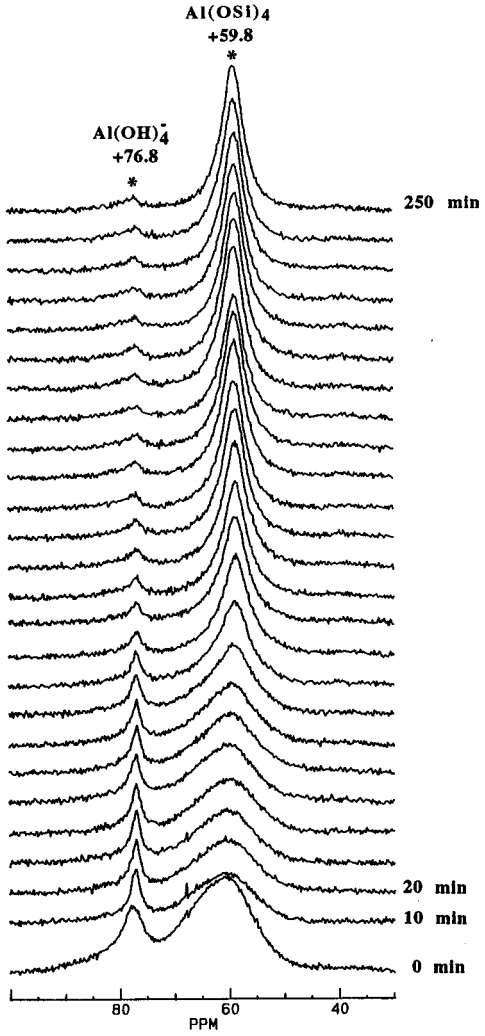

Figure 11. In situ ^{27}Al MAS NMR spectra on zeolite A synthesis from gel 2 at 65 °C (after 30 min of mixing).

sistent with previous studies on zeolite A[4,5] and that observed by Zhdanov et al. for zeolite X.[3] The crystal growth rate for gel 1 is finished after 150 min, but slow growth continues until 250 min while the gel 2 synthesis is completed after 120 min. Figure 12ii indicates that the initiation of crystallization is associated with reduction of free $[Al(OH)_4]^-$ ions. The aluminum concentrations of both supernatant liquid solutions of gels 1 and 2 are almost the same at completion of crystallization. The free aluminate concentration gradually decreases during the early part of crystallization (0−70 min) but more rapidly near the end of the crystallization (between 70 and 250 min for gel 1, between 70 and 150 min for gel 2). Rapid depletion of free aluminate occurs during the phase of rapid crystallization. A corresponding increase in the concentration of $Al(OSi)_4$ is observed in both cases. Both of these changes take place more gradually for gel 1 than gel 2.

Discussion

The ^{27}Si and ^{27}Al MAS NMR and XRD data give a coherent and consistent picture of the crystal growth of zeolite-A in the two different recipes:

(i) The final product is the same although the initial gel compositions are different for both recipes; gel 1 has more $[Si(OH)_4]$ and $[Al(OH)_4]^-$ than gel 2. This is consistent with the greater alkalinity and water content of the gel.

(ii) Crystal growth is associated with a decrease in the $w_{1/2}$ (Al_{Td}) (half-height width of the tetrahydrally coordinated alumina peak at +59 ppm), and increase in the formation of solid $Al(OSi)_4$ units and a decrease in the concentration of free $[Al(OH)_4]^-$ ions. It is also associated with the growth of an X-ray crystalline phase and an increase in the intensity of a ^{29}Si NMR resonance corresponding to zeolite 4A. Once crystal growth begins it is rapid and most of gel is transformed into crystalline zeolite within a short period of time.

(iii) The NMR spectra (both ^{29}Si and ^{27}Al) indicate that there is little change in the spectra during the period before crystal growth begins (30 min). This indicates that NMR is not sensitive enough to describe the early changes in the gel chemistry.

(iv) The ^{29}Si and ^{27}Al MAS NMR of gel 2 at all stages of the in situ synthesis do not indicate that there are NMR observable quantities of more complex soluble aluminosilicate or silicate species (so-called secondary building units). There has been considerable discussion in the literature concerning the formation of secondary

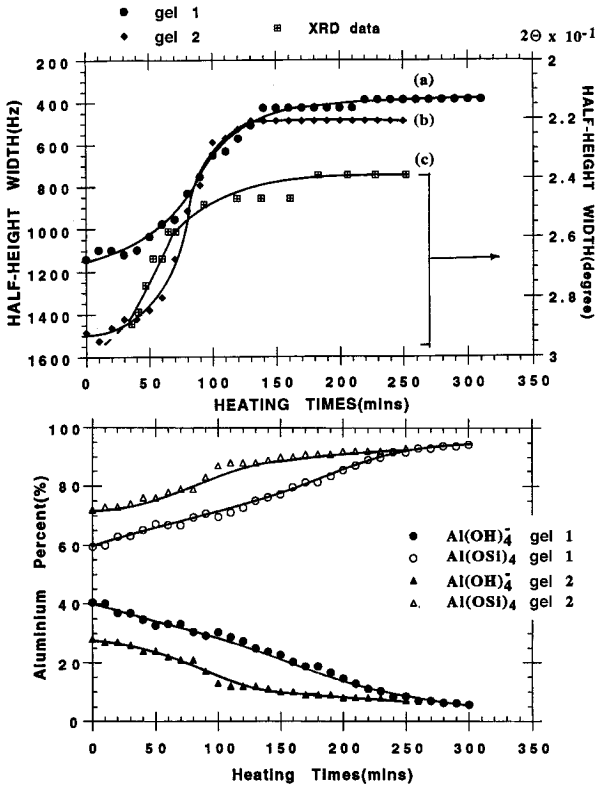

Figure 12. (i) Plots of the half-width of 59 ppm peak from ^{17}Al MAS NMR spectra against time for gels 1 and 2 and a plot of the XRD crystallinity measured from the 2θ −29.9° line against heating time. (ii) Curves of the aluminum percent vs heating time: in the liquid phase (top) and in the gel phase (bottom).

building units and their role in zeolite synthesis.[27] The only distinct species observed are amorphous $Al(OSi)_4$ units, a small amount of Q^0(Si) and $[Al(OH)_4]^-$, and the growing zeolite phase.

(v) The more concentrated gel (gel 2) gives a more rapid crystallization; this suggests that more nuclei are formed during the induction/nucleation period. This is reflected in the small size of the resultant crystals. In this case a more sudden depletion of Q^0(Si) and $[Al(OH)_4]$ ions is observed. This is consistent with their lower initial concentration in the zeolite gel solution.

(vi) The NMR data of the gel is tentatively assigned to $Si(OAl)_4$ units with a range of chemical shifts centered at approximately −85 ppm corresponding to a disordered matrix with wide range of T−O−T angles: the majority of the T−O−T angles are smaller than those observed for zeolite-A.[8,28] This suggests dramatic reorganization of the species present on crystallization.

Two models for crystallization have been proposed—one based on solution-phase transformation and the second based on a solid hydrogel transformation.[1] The above evidence supports a mechanism which is solution mediated via Q^0(Si) and $[Al(OH)_4]^-$ ions which are formed by rapid dissolution of the gel. Once formed, these units are rapidly deposited on the growing zeolite surface. It is postulated that much of this transformation occurs in the vicinity of the solid gel phase. In a recent paper Chen et al. use a modified population balance model to propose that growth at the surface of crystals is the rate-determining step.[7] For simplicity they proposed a model where half a pseudocell is precipitated at a time. However, their data are consistent with a mechanism of rapid deposition of monomeric aluminum and silicate ions.

Conclusions

This paper describes the use of solid state NMR for the in situ study of zeolite synthesis. For the zeolite A system we have been able to investigate the species present in the gel without need to remove or separate parts of the gel. It is clear that this technique is of considerable utility in studying in situ crystalline processes in zeolites when used in conjunction with information for other techniques. With the constant improvement in sensitivity and NMR probe and rotor design, it should be feasible to extend this approach to zeolitic systems which require hydrothermal crystallization conditions and which have different crystallization time scale. It should be possible to apply this technique to a range of zeolite systems of interest to build a more complete picture of speciation and growth behavior of a range of zeolitic materials.

Acknowledgment. We thank Unilever Research for support for Jimini Shi, Dr. Peter Graham for helpful discussions, and the referees for many constructive comments.

CM950028N

(27) Knight, C. T. G. *Zeolites* **1990**, *10*, 140−144.

(28) Klinowski, J. *Prog. NMR Spectrosc.* **1984**, *16*, 237−309.